



Channel flow LES with stochastic modeling of the subgrid acceleration

Mikhael Gorokhovski, Rémi Zamansky, Ivana Vinkovic

► To cite this version:

Mikhael Gorokhovski, Rémi Zamansky, Ivana Vinkovic. Channel flow LES with stochastic modeling of the subgrid acceleration. Studying Turbulence Using Numerical Simulation Databases - XII, Jul 2011, Stanford, United States. pp.377-386. hal-00683116

HAL Id: hal-00683116

<https://hal.science/hal-00683116>

Submitted on 27 Mar 2012

HAL is a multi-disciplinary open access archive for the deposit and dissemination of scientific research documents, whether they are published or not. The documents may come from teaching and research institutions in France or abroad, or from public or private research centers.

L'archive ouverte pluridisciplinaire **HAL**, est destinée au dépôt et à la diffusion de documents scientifiques de niveau recherche, publiés ou non, émanant des établissements d'enseignement et de recherche français ou étrangers, des laboratoires publics ou privés.

Channel flow LES with stochastic modeling of the subgrid acceleration

By M. Gorokhovski[†], R. Zamansky[†] AND I. Vinkovic[†]

In this paper, the non-filtered velocity field in a well-developed turbulent channel flow is simulated in the framework of LES-SSAM (stochastic subgrid acceleration model) approach. A novel stochastic SGS model is proposed. This model introduces explicitly the cross-channel correlation of subgrid velocity gradients and includes two parameters: the Reynolds number based on the friction velocity, and the channel half-width. The objective was to assess the capability of this model in comparison to the standard LES and to direct numerical simulation (DNS).

1. Introduction

The structure of well-developed turbulent wall layer in the channel flow is highly intermittent; close to the wall, the low-speed regions are interleaved with tiny zones of the high-speed motion. The main role in this intermittency is attributed to quasi-streamwise vortices formed in the near-wall layer (Kaftori *et al.* 1994; Adrian *et al.* 2000; Tomkins & Adrian 2003). Their anisotropic dynamics are Reynolds-number dependent. Sweeps from the outer layer toward the wall induce strong variations of the wall-normal velocity. The cross-channel correlation in the turbulent velocity field is amplified by merging of near-wall small-scale structures and their eruptions towards the outer region. (Jimenez *et al.* 2004; Toh & Itano 2005; Hutchins & Marusic 2007). While the large-eddy simulation (LES) of such flows may capture the near-wall flow physics (Moin & Kim 1982; Piomelli 1993; Perot & Moin 1995a 1995b), its accuracy greatly depends on details of the grid and of its resolution near the wall (Piomelli 1999). As shown by Baggett *et al.* (1997), the number of anisotropic modes to be resolved properly by LES in the near-wall region scales roughly as the square of the Reynolds number. Then for a high Reynolds number, the accurate prediction of turbulent wall layer requires CPU resources that are too expensive (Pope 2004). Among numerous approaches (reviewed, for example, in Meneveau & Katz 2000; Kerstein 2001; Piomelli & Balaras 2002; Sagaut 2002; Spalart *et al.* 2006) that aim to bypass such requirements, one of them consists in the combining of the LES at moderate resolution with the subgrid scale (SGS) model of the non-resolved turbulent motion. The majority of SGS models are focused on simulation of turbulent stresses generated by the non-resolved velocity field (Meneveau & Katz 2000; Domaradzki & Adams 2002; Park & Mahesh 2008). In these models the structure of subgrid flow is supposed to be independent of the Reynolds number, *i.e.*, to be not intermittent. The approaches of Schmidt *et al.* (2003) and of Kemenov & Menon (2007) go beyond computation of the filtered velocity field. The approach of Schmidt *et al.* (2003) is focused on the LES/ODT coupling (Kerstein 1999; Kerstein *et al.* 2001), providing for stochastic simulation of the fluctuating velocity field close to the wall. The approach of Kemenov & Menon (2007) is based on computation of the synthetic velocity field, as superposition of large-scale

[†] LMFA UMR 5509 CNRS Ecole Centrale de Lyon, France

and small-scale velocities. The last one is computed explicitly on subgrid scales by 1-D motion equation (in three directions), in which the pressure gradient is omitted.

While in a high-Reynolds number intermittent flow, the acceleration on small spatial scales is governed mainly by the pressure gradient (Monin & Yaglom 1981), the explicit resolution of the pressure gradient on subgrid scales is too difficult. Therefore the recently proposed approach by Sabelnikov *et al.* (2007) is focused directly on the stochastic modeling of the subgrid acceleration (LES-SSAM). In fact, for a given filter width, the non-resolved acceleration may be substantially greater than the resolved acceleration. In terms of classical Kolmogorovs scaling, this is seen from the following estimation: $(\bar{a}_k \bar{a}_k)/(a'_i a'_i) \approx (\eta/\Delta)^{2/3}$, where \bar{a}_k and a'_i represent accelerations, respectively, in resolved and non-resolved motions, Δ is the filter width, $\eta = L/Re_L^{3/4}$ is the Kolmogorovs scale, L is the integral turbulent scale, $Re_L = \sigma_\mu L/\nu$, and σ_μ denotes the root mean squared (rms) velocity. This argument from Sabelnikov *et al.* (2007) implies that in any SGS model, which is aimed to introduce the intermittency effects, the non-resolved acceleration must be a key variable. In the LES-SSAM approach, the non-filtered velocity field is simulated, instead of computation of the filtered velocity. This is done by computation of the instantaneous model equation, in which the local acceleration includes two parts. The first one represents the filtered total acceleration, corresponding to the classical LES approach. The second one is associated with the sub-grid acceleration, which is modeled as stochastic in time process, in lines of the Kolmogorov-Oboukhov 62 theory and experimental observations of Mordant (2001, 2004). The non-resolved velocity field, computed in this way, is updated in order to satisfy the continuity equation. Using this approach, the computed statistics of the Lagrangian acceleration in the stationary 3-D box turbulence reproduced the experimental observations of Mordant (2001, 2004): (i) non-Gaussian distribution with stretched tails; (ii) rapid de-correlation (of order of Kolmogorovs time) of acceleration with increasing of time lag; (iii) a long memory (of order of few integral times) of autocorrelation of the acceleration norm. This motivated us to further develop this approach for computation of a well-developed turbulent channel flow. During the CTR Summer Program, we proposed a novel stochastic subgrid scale (SGS) model of the non-resolved acceleration. The stochastic model introduces explicitly the cross-channel correlation of subgrid velocity gradients and includes two parameters: the Reynolds number based on the friction velocity, and the channel half-width. The objective was to assess the capability of this model in comparison to the standard LES and to direct numerical simulation (DNS). The LES-SSAM approach from Sabelnikov *et al.* (2007) is described in Sec. 2. The stochastic subgrid acceleration model is presented in Sec. 3. The results are discussed in Sec. 4.

2. Formulation of the LES-SSAM approach

The total instantaneous acceleration, governed by the Navier-Stokes equations, can be represented by the sum of two parts: $a_i = \bar{a}_i + a'_i$. The first part represents the spatially filtered total acceleration:

$$\bar{a}_i \equiv \frac{d\bar{u}_i}{dt} = -\frac{1}{\rho} \frac{\partial \bar{P}}{\partial x_i} + \nu \Delta \bar{u}_i \quad (2.1)$$

$$\frac{\partial \bar{u}_k}{\partial x_k} = 0 \quad (2.2)$$

where $\bar{a}_i = \frac{\partial \bar{u}_i}{\partial t} + \frac{\partial \overline{u_k u_i}}{\partial x_k}$, and $\overline{u_k u_i} = \overline{u_k} \overline{u_i} + \overline{u'_k u'_i} + \overline{u_k u'_i} + \overline{u'_k u_i}$ is the turbulent stress. The second part is associated with the total acceleration in the residual field:

$$a'_i \equiv \left(\frac{du_i}{dt} \right)' = -\frac{\partial P'}{\partial x_i} + \nu \Delta u'_i \quad (2.3)$$

$$\frac{\partial u'_k}{\partial x_k} = 0 \quad (2.4)$$

where $a'_i = \frac{\partial u'_i}{\partial t} + \frac{\partial u_k u_i - \overline{u_k u_i}}{\partial x_k}$. Both equations need to be modeled. In the LES-SSAM approach, eq. (2.1) is modeled in the framework of the classical LES approach, and eq. (2.3) is replaced by the following form:

$$\left(\frac{du_i}{dt} \right)' = -\frac{1}{\rho} \frac{\partial \hat{p}}{\partial x_i} + \hat{a}'_i \quad (2.5)$$

Here \hat{a}'_i is considered as a stochastic variable governed by presumed stochastic process, and the pressure \hat{p} guarantees the velocity vector to be solenoidal. A synthetic velocity field corresponding to the sum of two modeled accelerations (filtered and residual) is considered as an approximation of the non-filtered velocity field. The resulting model equation writes:

$$\frac{\partial \hat{u}_i}{\partial t} + \hat{u}_k \frac{\partial \hat{u}_i}{\partial x_k} = -\frac{1}{\rho} \frac{\partial \hat{p}}{\partial x_i} + \frac{\partial}{\partial x_k} (\nu + \nu_{turb}) \left(\frac{\partial \hat{u}_i}{\partial x_k} + \frac{\partial \hat{u}_k}{\partial x_i} \right) + \hat{a}'_i \quad (2.6)$$

where pressure \hat{p} is governed by the continuity equation:

$$\frac{\partial \hat{u}_i}{\partial x_k} = 0 \quad (2.7)$$

and ν_{turb} is given by the Smagorinsky subgrid model.

3. A stochastic model of the non-resolved acceleration

In the modeling of the non-resolved acceleration, three main assumptions are as follows. Following Gorokhovski & Chtab (2007) and Sabelnikov *et al.* (2007), the first proposal is to separate the characteristic times in variation of the subgrid acceleration vector. The fast process is associated with the rapid change of its orientation. The slow process is attributed to the stochastic relaxation of the modulus of acceleration. Then the non-resolved acceleration is written as:

$$\hat{a}'_i = |a|(t) e_i(t) \quad (3.1)$$

$$\langle e_i(t) e_j(t + \Delta t) \rangle = 0$$

where $e_i(t)$ is a unit vector with direction defined at each time step by two random angles $0 < \beta < \pi$ and $0 < \theta < 2\pi$; and $|a|(t)$ is modulus of the non-resolved acceleration. The second proposal is to emulate the modulus of the non-resolved acceleration by the product of the mean velocity increment in the wall-normal direction and the frequency of its variation, f ; the last one is considered as stochastic variable

$$|a|(t) = \Delta \langle \bar{S} \rangle f. \quad (3.2)$$

Here $\bar{S} \equiv (2S_{ij}S_{ij})^{1/2}$ is the characteristic filtered rate of strain. The third assumption concerns the stochastic evolution process for f from the wall to the outer flow. Let us

introduce the evolution parameter, τ , using the normal to the wall distance, y :

$$\begin{aligned}\tau &= -\ln\left(\frac{H-y}{H}\right) \\ y = 0 : \tau &= 0 \\ y = H : \tau &= \infty\end{aligned}\tag{3.3}$$

where H is the channel half-width. The near-wall region is characterized by strong velocity gradients (high values of f), which are decreasing in mean toward the outer flow through the highly intermittent boundary layer. Thereby we assumed that with increasing of the normal distance from the wall, the frequency f is changing by a random independent multiplier α ($0 < \alpha < 1$), governed by distribution $q(\alpha)$, $\int_0^1 q(\alpha)d\alpha = 1$, which is principle unknown. In other words, we apply the fragmentation stochastic process under scaling symmetry for the frequency f . The Fokker-Planck equation for the normalized distribution function $G(f, \tau)$, corresponding to this process, is (Gorokhovski & Saveliev 2008):

$$\frac{\partial G(f, \tau)}{\partial \tau} = -\langle \ln \alpha \rangle \frac{\partial}{\partial f} f G + \langle \ln^2 \alpha \rangle \frac{\partial}{\partial f} f \frac{\partial}{\partial f} f G \tag{3.4}$$

where $\int_0^1 G(f)df = 1$, $\langle \ln^k \alpha \rangle = \int_0^1 q(\alpha) \ln^k \alpha d\alpha$; $k = 1, 2$. From eq. (3.4), we derive the following stochastic equation in the Ito interpretation:

$$df = [\langle \ln \alpha \rangle + \langle \ln^2 \alpha \rangle / 2] f d\tau + \sqrt{\langle \ln^2 \alpha \rangle / 2} f dW(\tau) \tag{3.5}$$

where $dW(\tau)$ is the Wiener process and $[dW(\tau)]^2 = 2d\tau$. In the present paper, parameters are chosen in the following form:

$$-\langle \ln \alpha \rangle = \langle \ln^2 \alpha \rangle = \ln(Re_+) \tag{3.6}$$

where Re_+ is the Reynolds number, based on the friction velocity U_+ . Equations (3.3)–(3.6) constitute the random path of the frequency from the wall toward the center-line. The starting condition, $\tau = 0$, for this stochastic process (the first grid cell on the wall) is given as follows. We introduce the mean value of frequency $f_+ = \lambda/U_+$, where λ is determined, as a Taylor-like scale, which can be estimated by the Kolmogorovs scaling in the framework of definitions of wall parameters. The Reynolds number, based on friction velocity, is $Re_+ = U_+ H / \nu = H / y_0 \approx Re_H^{3/4}$ where y_0 is the thickness of the laminar layer, and Re_H is the Reynolds number based on the center-line velocity. One then yields: $\lambda \approx H Re_H^{-1/2} \approx H Re_+^{-2/3}$. Similar to Kolmogorov-Oboukhov 62, the starting condition for random path (3.5) is sampled from the stationary log-normal distribution of f/f_+ :

$$\begin{aligned}P_0(f/f_+) &= \frac{f_+}{f\sqrt{2\pi\sigma^2}} e^{-\frac{(\ln(f/f_+) - \mu)^2}{2\sigma^2}} \\ \sigma^2 &= \ln Re_+^{2/3} \\ \mu &= -\frac{1}{2}\sigma^2\end{aligned}\tag{3.7}$$

Two ensembles of realizations of eq. (3.5)–(3.7), are presented in Fig. 1, in the near-wall region, $y^+ = 5$ and in the outer flow $y^+ = 400$. A highly intermittent and intensive process is seen on the left, while on the right, the long small-frequency sequences are accompanied

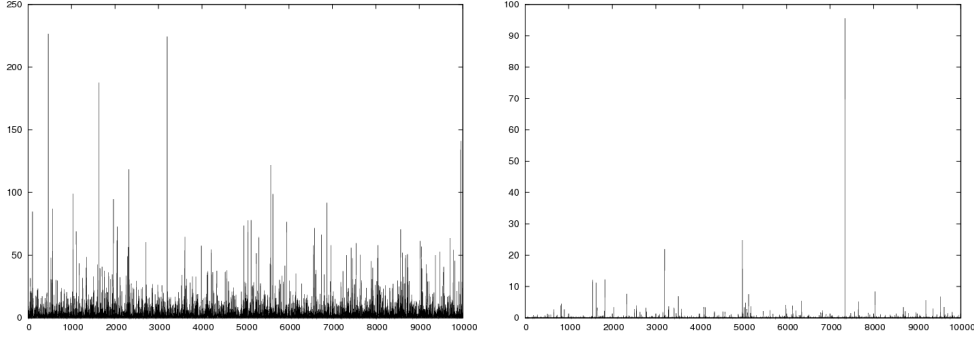


FIGURE 1. Frequency realizations by (3.5)-(3.7) at $y^+ = 5$ (on the left) and $y^+ = 400$ (on the right).

by very rare events of the high frequency (this may be attributed to ejection events of small scale eddies toward the outer flow).

4. Numerical results and comparison

The computations of the channel flow are performed using the pseudo-spectral method with integration in time by the explicit Adam-Basforth algorithm for convective terms, and by the implicit Crank-Nicholson algorithm for diffusion terms. A skew-symmetric form is used for non-linear terms in order to ensure the conservation of energy. The periodic boundary condition in the streamwise and spanwise directions, and no-slip boundary condition on the wall have been applied. The numerical approach is very similar to one from Piomelli (1993, 1999). When the standard LES was performed, we used the Van-Driest wall-damping function. In the LES-SSAM and in LES computations, the computational mesh was $64 \times 64 \times 64$, and the box size was $3\pi H \times 2H \times \pi H$ for the streamwise, wall-normal and spanwise directions, respectively. So, in the wall unities, for $Re_+ = 590$, the cell size is ranging from $86 \times 0.7 \times 29$ at the wall, to $86 \times 28 \times 28$ near the center-line. For the DNS computation, the mesh was $384 \times 256 \times 384$, and the box size was $3/2\pi H \times 2H \times 3/4\pi H$ for the streamwise, wall-normal and spanwise directions, respectively. The results from three approaches, LES-SSAM, classical LES and DNS, are compared. Figures 2 and 3 show the mean streamwise velocity profile and the standard deviation of the velocity fluctuation. It is seen that the LES-SSAM approach improves notably the predictions (less visible for v_{rms}^+). Using three approaches, we compare in Fig. 4 the computation of turbulent and viscous stresses, $\tau_{turb} = -\rho\langle u'v' \rangle$ and $\tau_{visc} = -\rho\nu\langle \frac{\partial u}{\partial y} \rangle$, respectively. The results are presented as ratios $\tau_{turb}/(\tau_{turb} + \tau_{visc})$ and $\tau_{visc}/(\tau_{turb} + \tau_{visc})$. Here again the advantage of the LES-SSAM approach *vs.* the classical LES is explicitly seen. The LES-SSAM approach with the model proposed also provides a better representation of flow in the near-wall region. This is demonstrated in Figs. 5 and 6, where the longitudinal spectra (for two distances from the wall, $y^+ = 5$ and $y^+ = 20$) and the longitudinal spatial autocorrelation for velocity in the near-wall layer ($y^+ = 2.8$) are presented. The last figures (Figs. 7 and 8) show distributions of the acceleration in comparison with DNS, and with the standard LES. It is seen that in agreement with the DNS, the distributions for both components of the acceleration, obtained by the LES-SSAM, expose the stretched tails, as a manifestation of intermittency.

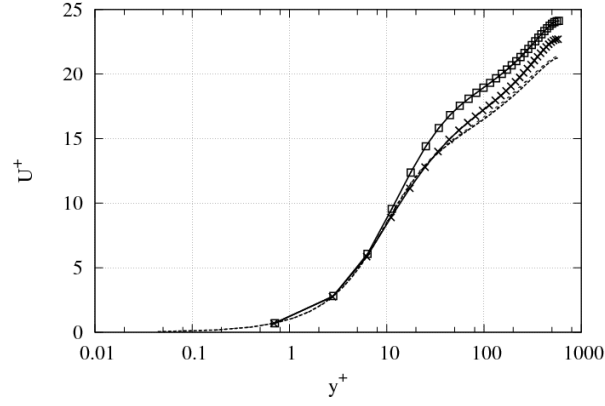


FIGURE 2. Streamwise mean velocity, $Re_+ = 590$. Square: LES; cross: LES-SSAM; dash: DNS; dots: DNS Mother *et al.* 1999.

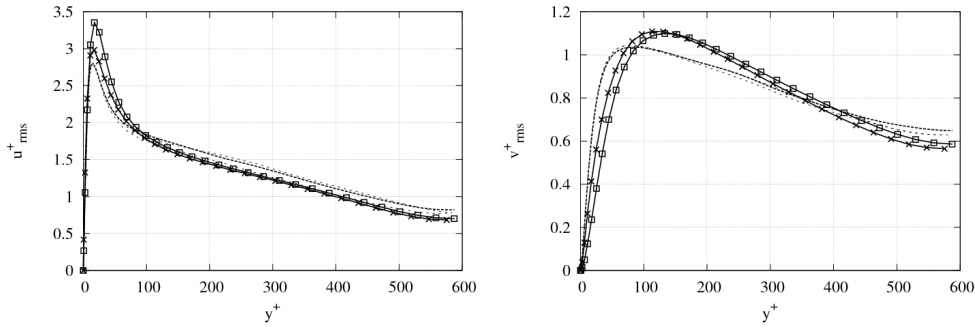


FIGURE 3. Rms of streamwise (on the left) and of normal (on the right) velocity, $Re_+ = 590$. Square: LES; cross: LES-SSAM; dash: DNS; dots: DNS Mother *et al.* 1999.

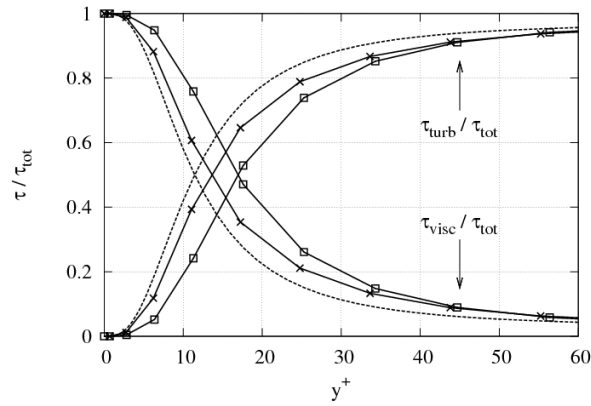


FIGURE 4. Fractions of turbulent $\tau_{turb} = -\rho\langle u'v' \rangle$ and viscous $\tau_{visc} = -\rho\nu\langle \frac{\partial u}{\partial y} \rangle$ stresses compared to the total one $\tau_{tot} = \tau_{visc} + \tau_{turb}$. $Re_+ = 590$. Square: LES; cross: LES-SSAM; dash: DNS.

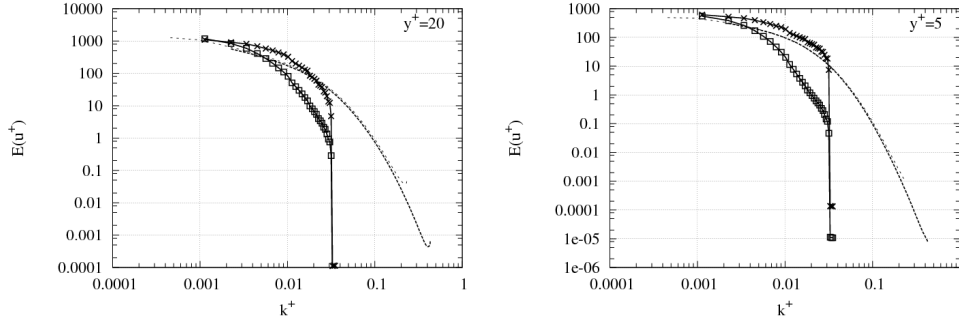


FIGURE 5. Normalized longitudinal 1-D spectra of streamwise velocity for two distances normal to the wall : $y^+ = 20$ and $y^+ = 5$, $Re_+ = 590$. Square: LES; cross: LES-SSAM; dash: DNS; dots: DNS Del Alamo *et al.* 2004.

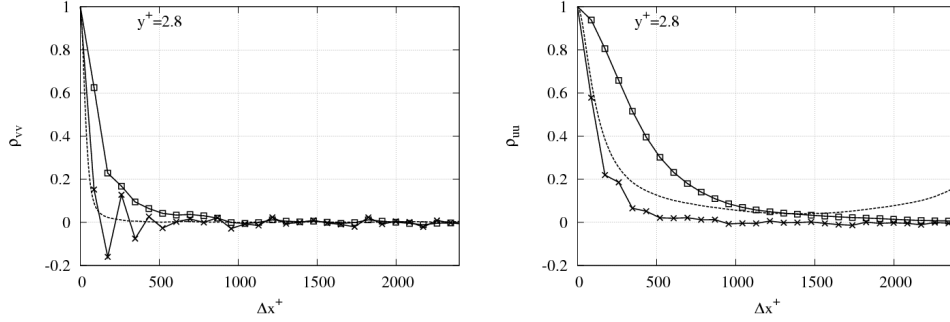


FIGURE 6. Longitudinal correlation of streamwise, normal and spanwise velocity, respectively, at $y^+ = 2.8$. $Re_+ = 590$. Square: LES; cross: LES-SSAM; dash: DNS.

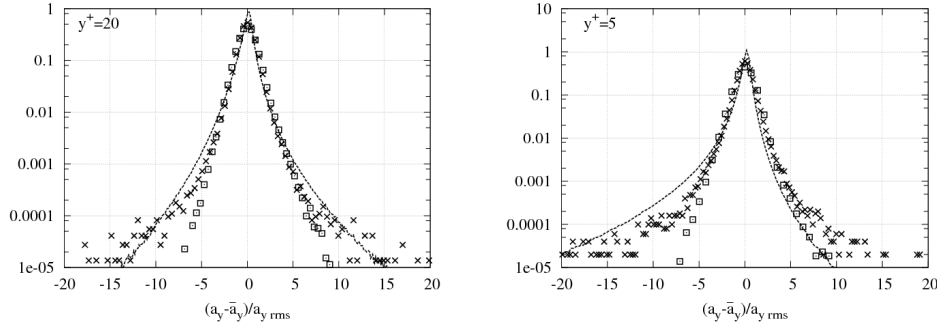


FIGURE 7. Distribution of normal component of acceleration for two distances to the wall : $y^+ = 20$ and $y^+ = 5$. Square: LES; cross: LES-SSAM; dash: DNS.

5. Conclusion

In the framework of the LES-SSAM approach, the new SGS model is proposed in order to represent the intermittency effects in the near-wall region of a high-Reynolds number channel flow. The assessment of this model is performed by comparison of computation with the DNS ($Re_+ = 590$). This comparison shows explicitly the improvements of

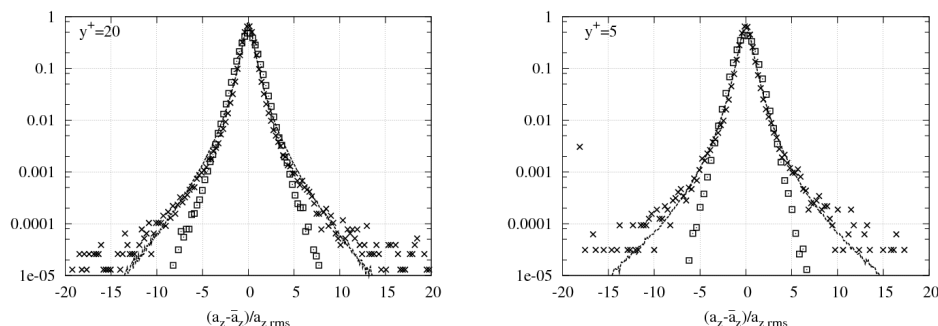


FIGURE 8. Distribution of spanwise component of acceleration for two distances to the wall : $y^+ = 20$ and $y^+ = 5$. Square: LES; cross: LES-SSAM; dash: DNS.

predictions provided by the new model. Future computation and analyses will investigate whether this is also the case for the higher Reynolds number.

REFERENCES

- ADRIAN, R. J., MEINHART, C. D. & TOMKINS, C. D. 2000 Vortex organization in the outer region of the turbulent boundary layer. *J. Fluid Mech.* **422**, 1–54.
- BAGGETT, J. S., JIMENEZ, J. & KRAVCHENKO A. G. 1997 Resolution requirements for large-eddy simulations of shear flows. *Annual Research Briefs 1997*, Center for Turbulence Research, Stanford University, Palo Alto, California, p. 51.
- DEL ALAMO, J. C., JIMENEZ, J., ZANDONADE, P. & MOSER, R. D. 2004 Scaling of the energy spectra of turbulent channels. *J. Fluid Mech.* **500**, 135–144.
- DOMARADZKI, J. A. & ADAMS, N. A. 2002 Direct modelling of subgrid scales of turbulence in large eddy simulations. *JOT* **3**, 0–24.
- GOROKHOVSKI, M. & CHTAB, A. 2007 LES of Lagrangian statistics in homogeneous stationary turbulence; application of universalities under scaling symmetry at sub-grid scales. In *Complex Effects in Large Eddy Simulation* Lecture Notes in Computational Science and Engineering, Springer, Moin P. *et al.* (eds), **56**, 63–75.
- GOROKHOVSKI M. A. & SAVELIEV V. L. 2008 Statistical universalities in fragmentation under scaling symmetry with a constant frequency of fragmentation. *J. Phys. D Appl. Phys.* **41**, 085405.
- HUTCHINS, N. & MARUSIC, I. 2007 Evidence of very long meandering features in the logarithmic region of turbulent boundary layers. *J. Fluid Mech.* **579**, 1–28.
- JIMENEZ, J., DEL ALAMO, J. C. & FLORES O. 2004 The large-scale dynamics of near-wall turbulence. *J. Fluid Mech.* **505**, 179–199.
- KAFTORI, D., HETSRONI, G. & BANERJEE, S. 1994 Funnel-shaped vortical structures in wall structures. *Phys. Fluids* **6** (9), 3035–3050.
- KEMENOV, K. A. & MENON, S. 2006 Explicit small-scale velocity simulation for high-Re turbulent flows. *J. Comput. Phys.* **220**, 290–311.
- KEMENOV, K. A. & MENON, S. 2007 Explicit small-scale velocity simulation for high-Re turbulent flows. Part II: Non-homogeneous flows. *J. Comput. Phys.* **222**, 673–701.
- KERSTEIN, A. 2002 One-dimensional turbulence: A new approach to high-fidelity subgrid closure of turbulent flow simulations. *Computer Physics Communications* **148**, 1–16.

- KERSTEIN, A. R., ASHURST, W. T., WUNSCH, S. & NILSEN, V. 2001 One-dimensional turbulence: vector formulation and application to free shear flows. *J. Fluid Mech.* **447**, 85–109.
- KERSTEIN, A. R. 1999 One-dimensional turbulence: model formulation and application to homogeneous turbulence, shear flows, and buoyant stratified flows. *J. Fluid Mech.* **392**, 277–334.
- MENEVEAU, C. & KATZ, J. 2000 Scale-invariance and turbulence models for large-eddy simulation. *Annu. Rev. Fluid Mech.* **32**, 1–32.
- MOIN, P. & KIM, J. 1982 Numerical investigation of turbulent channel flow. *J. Fluid Mech.* **118**, 341–377.
- MONIN, A. S. & YAGLOM, A. M. 1981 *Statistical Fluid Mechanics: Mechanics of Turbulence*. MIT Press.
- MORDANT, N., METZ, P., MICHEL, O. & PINTON, J.-F. 2001 Measurement of Lagrangian velocity in fully developed turbulence. *Phys. Rev. Lett.* **21**, 214501-1.
- MORDANT, N., LEVEQUE, E. & PINTON, J.-F. 2004 Experimental and numerical study of the Lagrangian dynamics of high Reynolds turbulence. *New Journal of Physics* **6**, 116.
- MOSER, R. D., KIM, J. & MANSOUR, N. N. 1999 Direct numerical simulation of turbulent channel flow up to $Re_\tau = 590$. *Phys. Fluids* **11** (4), 943–945.
- PARK, N. & MAHESH K. 2008 A velocity-estimation subgrid model constrained by subgrid scale dissipation. *J. Comput. Phys.* **227**, 4190–4206.
- PEROT, B. & MOIN, P. 1995a Shear-free turbulent boundary layers, part 1: Physical insight into near wall turbulence. *J. Fluid Mech.* **295**, 199.
- PEROT, B. & MOIN, P. 1995b Shear-free turbulent boundary layers. Part 2. New concepts for Reynolds stress transport equation modelling of inhomogeneous flows. *J. Fluid Mech.* **295**, 229–245.
- PIOMELLI, U. 1993 High Reynolds number calculations using the dynamic subgrid-scale stress model. *Phys. Fluids A* **5** (6), 1484–1490.
- PIOMELLI, U. 1999 Large-eddy simulation: achievements and challenges. *Progress in Aerospace Science* **35**, 335–362.
- PIOMELLI, U. & BALARAS, E. 2002 Wall-layer models for large-eddy simulations, *Ann. Rev. Fluid Mech.* **34**, 349.
- POPE, S. B. 2000 *Turbulent Flows*. Cambridge University Press.
- POPE, S. 2004 Ten questions concerning the large-eddy simulation of turbulent flows. *New Journal of Physics* **6** (35), 1–24.
- SABELNIKOV, V., CHTAB, A. & GOROKHOVSKI, M. 2007 The coupled LES - subgrid stochastic acceleration model (LES-SSAM) of a high Reynolds number flows. *Advances in Turbulence XI*, 11th EUROMECH European Turbulence Conference, June 25–28, 2007, Porto, Portugal, Springer Proceedings in Physics, Vol. **117**, Palma, J. M. L. M.; Silva Lopes, A. (Eds.), p. 209–211
- SAGAULT, P. 2002 *Large Eddy Simulation for Incompressible Flows: An introduction*. Springer Verlag, (second ed.).
- SCHMIDT, R.C., KERSTEIN, A. R., WUNSCH, S. & NILSEN V. 2003 Near-wall LES closure based on one-dimensional turbulence modelling. *J. Comput. Phys.* **186**, 317–355.
- SPALART, P. R., DECK, S., SHUR, M. L., SQUIRES, K. D., STRELETS, M. KH. &

- TRAVIN, A. 2006 A new version of detached-eddy simulation, resistant to ambiguous grid densities. *Theor. Comput. Fluid Dyn.* **20**, 181–195.
- TOH, S. & ITANO, T. 2005 Interaction between a large-scale structure and near-wall structures in channel flow. *J. Fluid Mech.* **524**, 249–262.
- TOMKINS, C. D. & ADRIAN, R. J. 2003 Spanwise structure and scale growth in turbulent boundary layers. *J. Fluid Mech.* **490**, 37–74.